Supplementary Information

Plant Perception of *β*-aminobutyric acid is mediated by an aspartyl tRNA synthetase

Estrella Luna, Marieke van Hulten, Yuhua Zhang, Oliver Berkowitz, Ana López, Pierre Pétriacq, Matthew A. Sellwood, Beining Chen, Mike Burrell, Allison van de Meene, Corné M.J. Pieterse, Victor Flors, and Jurriaan Ton

Supplementary Results

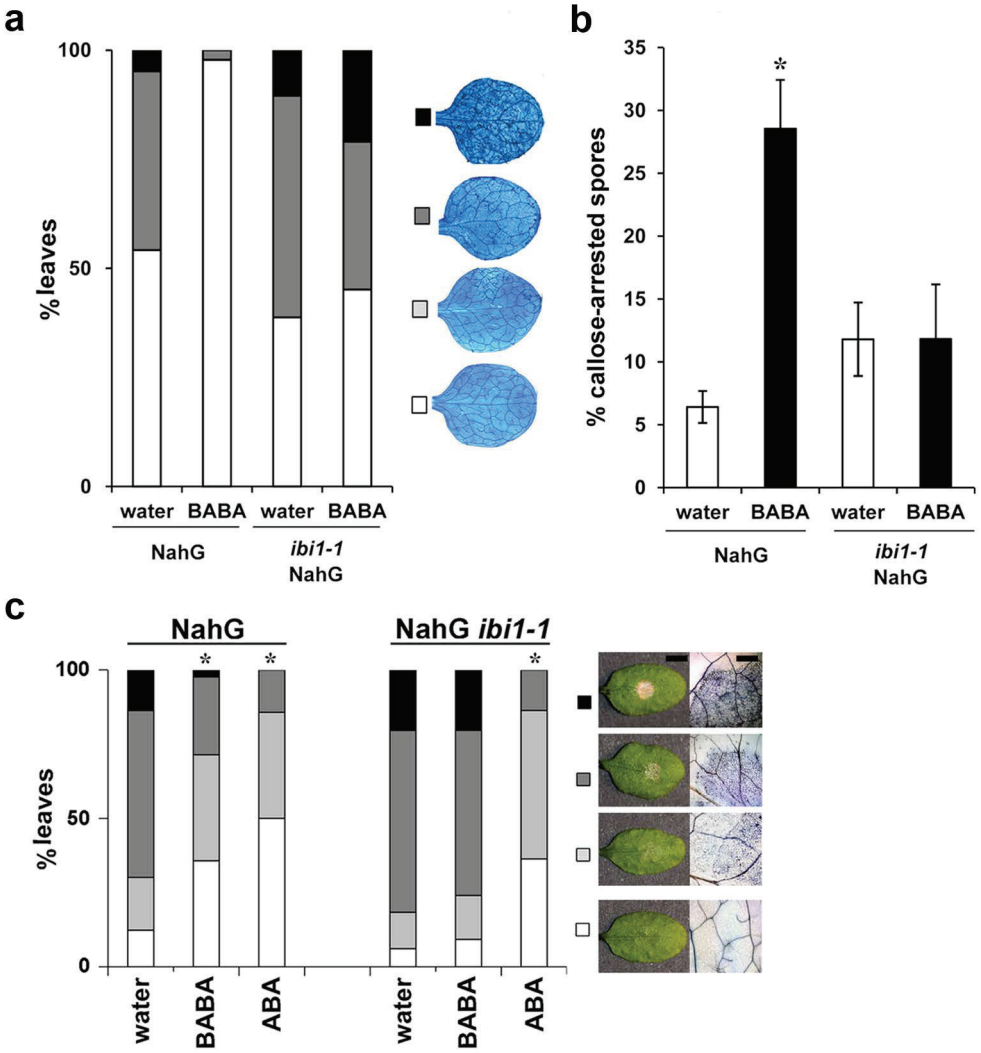

Supplementary Figure 1: IBI1 controls SA-independent BABA-induced resistance against biotrophic and necrotrophic pathogens. (a) The *ibi1-1* mutation in the genetic background of SA-deprived NahG blocks induced resistance against biotrophic *H. arabidopsidis* WACO9 after root treatment with BABA (150 µM). Insets show different classes of pathogen colonization. **(b)** Relative levels of arrested *H. arabidopsdis* WACO9 spores in NahG and NahG *ibi1-1* after treatment with water or BABA (150 µM). Data represent mean percentages (± SEM) of conidiospores, from which the emerging germ tubes were encapsulated in callose. Asterisk indicates a statistically significant difference in comparison to water-treated plants according to a Student's t-test (p<0.05, n=15) and a Binomial test (p<0.05). **(c)** Levels of induced resistance against necrotrophic *Plectosphaerella cucumerina* in NahG and NahG *ibi1-1* after root treatment with BABA (150 µM) or ABA (75 µM). Insets show different classes of lesion severity and pathogen colonization/cell death. Asterisks indicate statistically significant differences in class distribution relative to water-treated control plants (χ2 test or Fisher's exact test, p<0.01, n=50-100). Scale bars= 4 mm (left panel) and 0.75 mm (right panel)

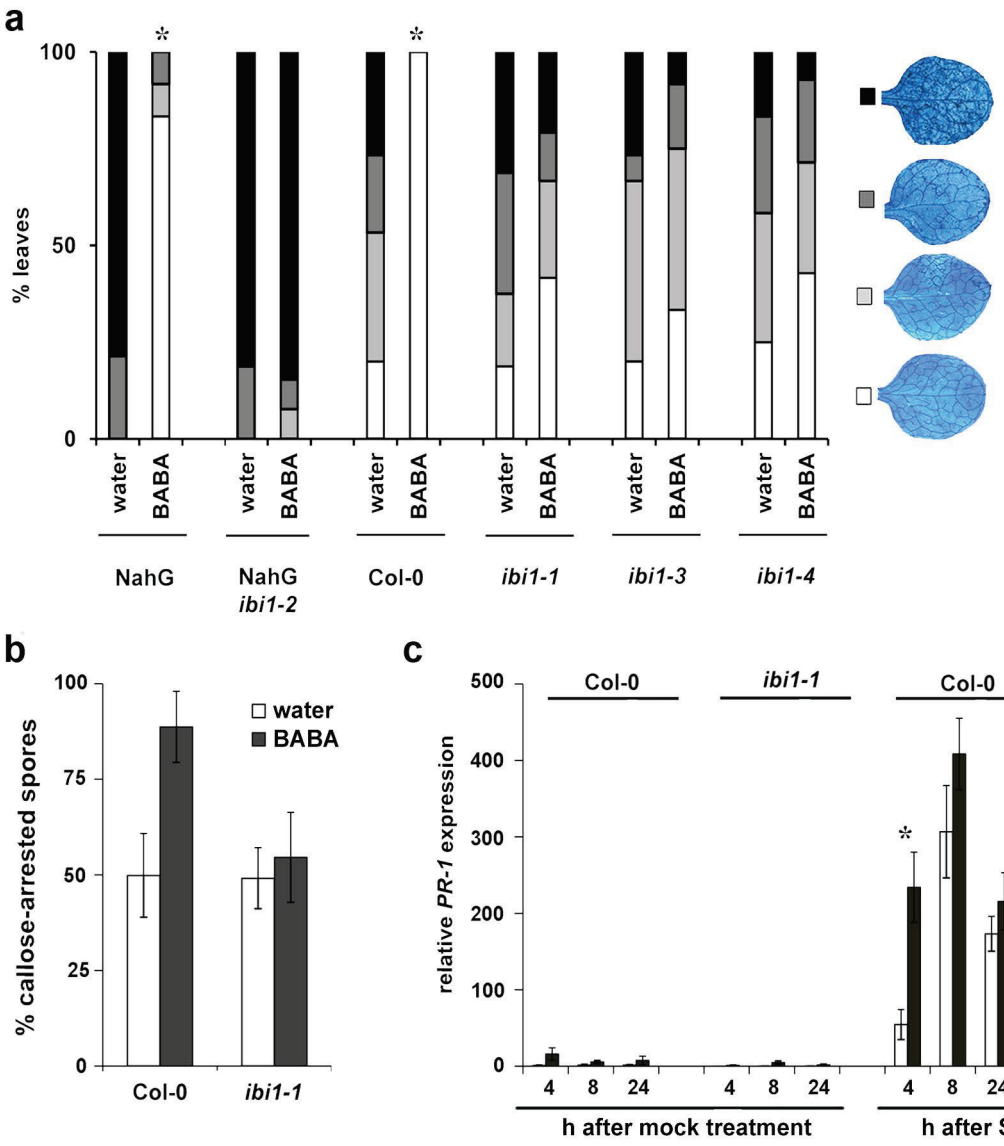

Supplementary Figure 2: Characterization of the *ibi1* mutant. (a) Independent *ibi1* mutations in the genetic background of both SA-deprived NahG and SA-producing Col-0 block induced resistance against *H. arabidopsidis* WACO9 after root treatment with BABA (150 µM). Insets show different classes of pathogen colonization; asterisks indicate statistically significant differences in class distribution relative to water-treated plants (Fisher's exact test, $p<0.01$, n=50-100). **(b)** Relative levels of arrested *H. arabidopsidis* WACO9 spores in Col-0 and *ibi1-1* after treatment with water or BABA (150 µM). Data represent mean percentages (± SEM) of conidiophores, from which the emerging germ tubes were encapsulated in callose. **(c)** *PR1* transcript accumulation in water- and BABA-treated (150 µM) Col-0 and *ibi1-1* at different hours (h) after spraying the leaves with mock solution or 0.5 mM SA. **(d)** *PR1* transcript accumulation in water- and BABA-treated (150 µM) Col-0 and *ibi1-1* at 2 days after mock/*H. arabidopsidis* WACO9 inoculation. Data in **(c)** and **(d)** represent average gene expression values (± SEM) relative to mock-treated Col-0. Asterisk indicates statistically different levels of *PR1* induction between water- and BABA-treated plants (Student's t-test, $p<0.05$, n=3)

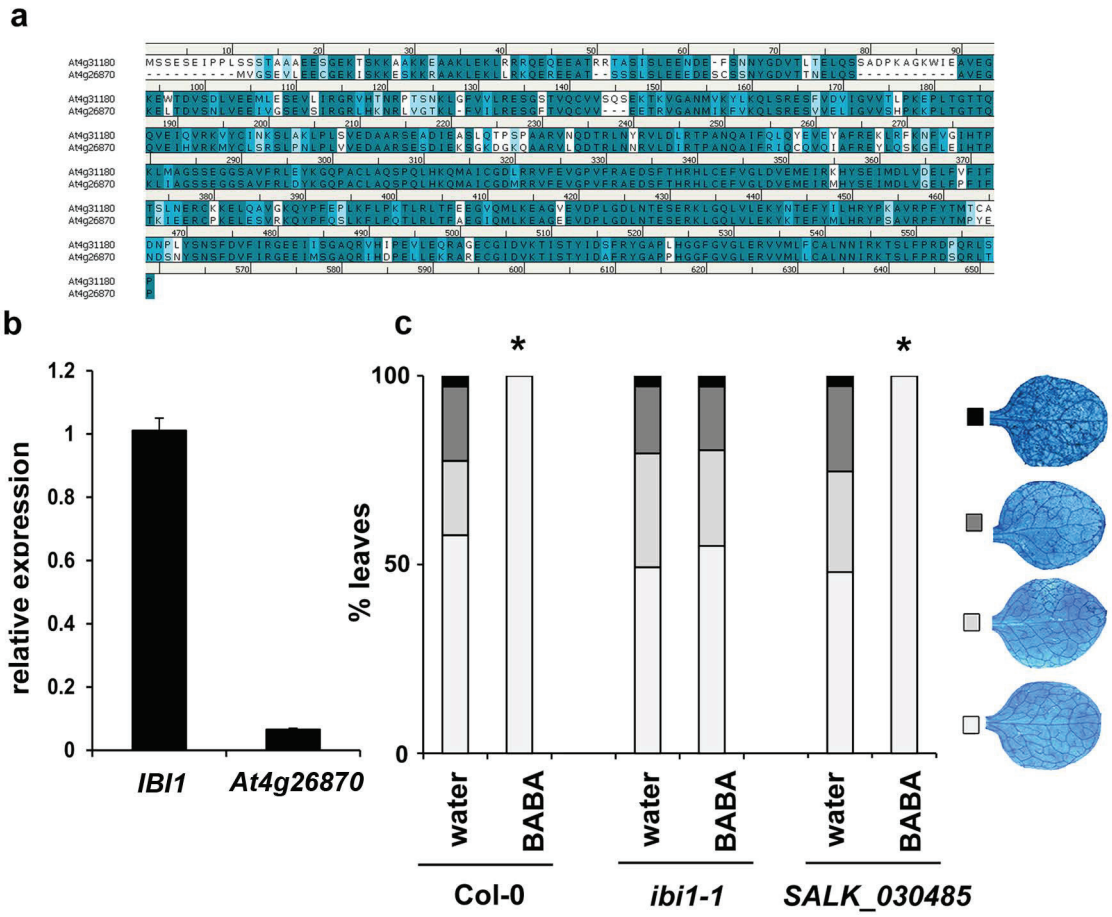

Supplementary Figure 3. The IBI1 homologue At4g26870 does not regulate BABA-induced resistance. (a) Protein alignments between IBI1 and At4g26870. Dark blue shades indicate identical amino acid sequences; light blue shades indicate similar amino acid sequences. **(b)** Basal transcription of *IBI1* and *At4g26870* in wild-type plants (Col-0). Data represent average values of relative gene expression (± SEM; n=3). **(c)** Levels of induced resistance against *H. arabidopsidis* WACO9 after root treatment with BABA (150 µM) in Col-0, *ibi1-1* and a T-DNA insertion mutant of *At4g26870* (*SALK_030485*). Insets show different classes of pathogen colonization; asterisks indicate statistically significant differences in class distribution relative to water-treated plants (Fisher's exact test, p<0.01, n=50-100).

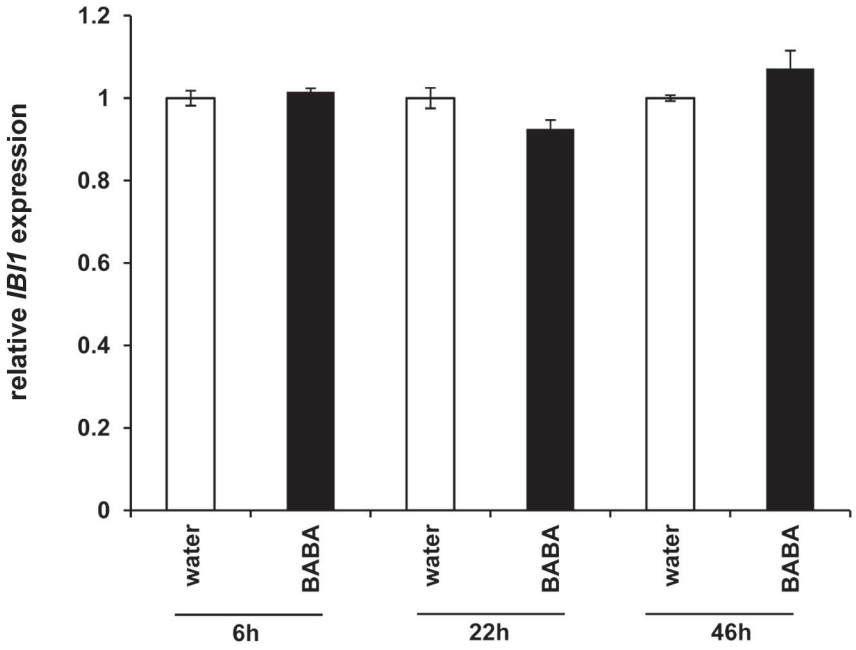

Supplementary Figure 4. The *IBI1* gene is transcriptionally unresponsive to BABA. Data represent average gene expression values (± SEM, n=3) relative to water-treated Col-0 at different hours (h) after treatment with BABA (150 µM).

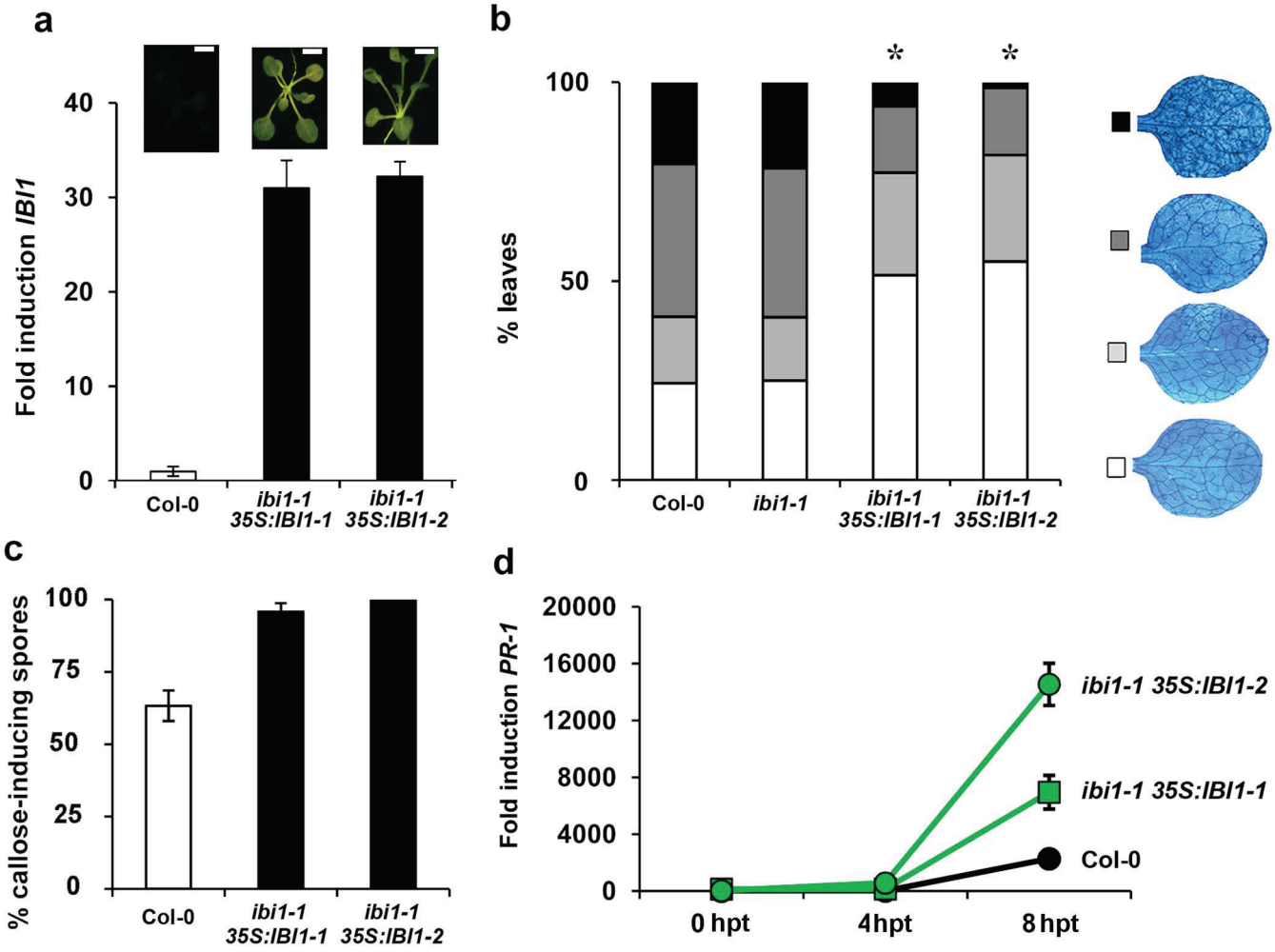

Supplementary Figure 5. Characterization of transgenic *ibi1-1 35S:IBI1:YFP* lines. (a) Levels of *IBI1* transcription in Col-0 in comparison to two independent *35S:IBI1:YFP* lines in the genetic background of the *ibi1-1* mutant. Shown are average transcript levels of *IBI1* (± SEM, n=3) relative to un-treated Col-0 plants. Insets show YFP fluorescence of transgenic seedlgins. Scale bar= 3 mm. **(b)** Levels of basal resistance against *H. arabidopsidis* WACO9 in Col-0, *ibi1-1* and two independent *ibi1-1 35S:IBI1:YFP* lines at 5 dpi. Insets show different classes of pathogen colonization; asterisks indicate statistically significant differences in class distribution relative to water-treated wild-type plants (Fisher's exact test, $p<0.01$, n=50-100). **(c)** Relative levels of arrested *H. arabidopsdis* WACO9 spores in Col-0 and *ibi1-1 35S:IBI1:YFP* lines after treatment with water or BABA (150 µM). Data represent mean percentages (± SEM, n=10) of conidiospores, from which the emerging germ tubes were encapsulated in callose. **(d)** *PR1* transcript accumulation in Col-0 and *ibi1-1 35S:IBI1:YFP* lines at 4 and 8 hours post SA treatment (hpt; 0.5 mM). Values indicate average levels of *PR1* induction relative to average transcript levels in Col-0 plants before SA application.

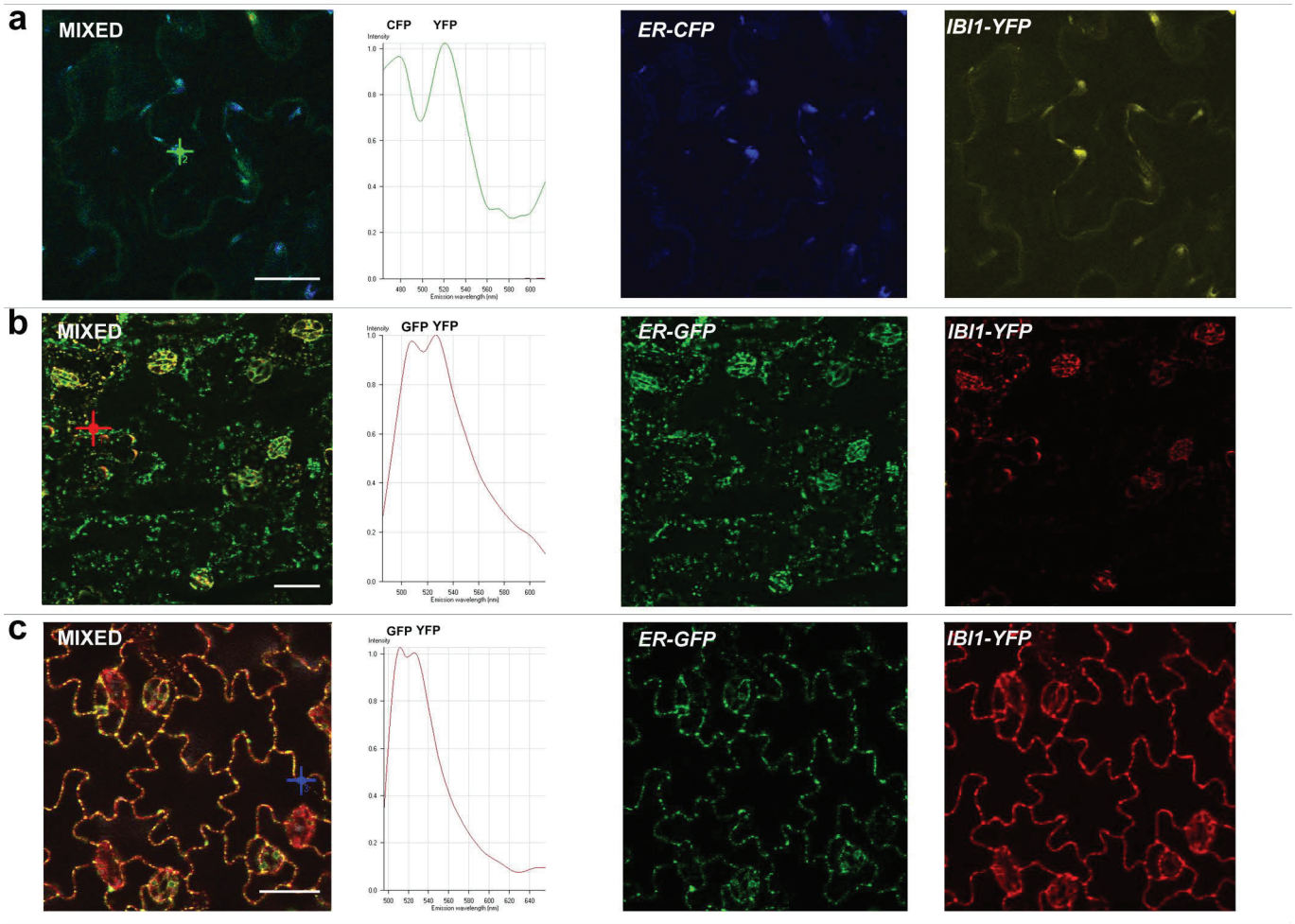

Supplementary Figure 6. Co-localization of IBI1-YFP with ER-CFP (a) or ER-GFP (b and c) in un-primed plants. (a) YFP and CFP fluorescence in cotyledon cells of 2-week-old F1 progeny (*35S:IBI1:YFP-1 x ER-ck*), scanned with a multi-photon laser. Scale bar = 10 µm. **(b)** YFP and GFP fluorescence in cells of an epidermal peel from leaves of 5-week-old F1 progeny (*ibi1-1 35S:IBI1:YFP-1 x ER-gk*), scanned with a multi-photon laser. Scale bar = 50 µm. **(c)** YFP and GFP fluorescence in cotyledon cells of 2-week-old F1 progeny (*ibi1-1 35S:IBI1:YFP-1 x ER-gk*), scanned with a single-photon laser. Scale bar = 50 µm. Mixed photographs (left) show merged fluorescence spectra (centre) at the emission range of both fluorescent proteins from the targeted region (indicated by a cross). Un-mixed photographs (right) show fluorescence from each of the two fluorescent proteins. YFP fluorescence in analyses of F1 progeny from *ibi1-1 35S:IBI1:YFP-1 x ER-gk* in (**a**) and (**b**) has been adjusted to red to facilitate distinction with GFP fluorescence.

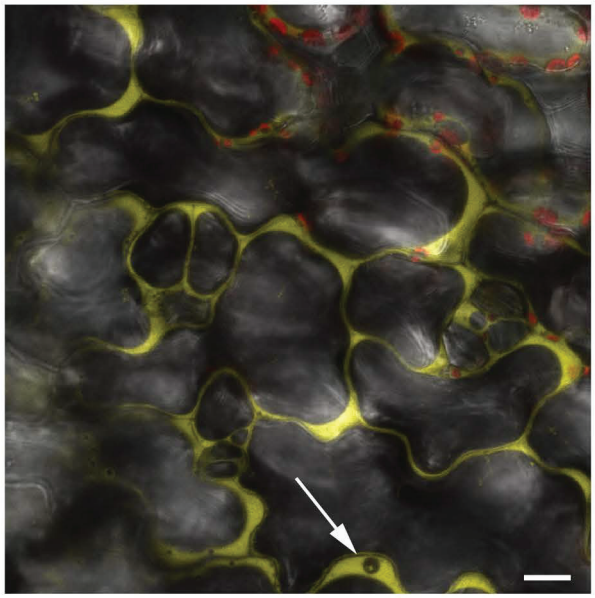

Supplementary Figure 7. Localisation of IBI1-YFP in peripheral cytoplasm of epidermal leaf cells from BABA-treated *ibi1-1 35S:IBI1:YFP-1* plants (150 µM) at 5 dpi with *H. arabidopsidis*. The arrowhead points to a nucleus that is fully surrounded by yellow fluorescence from IBI1-YFP. Scale bar = 15 µm

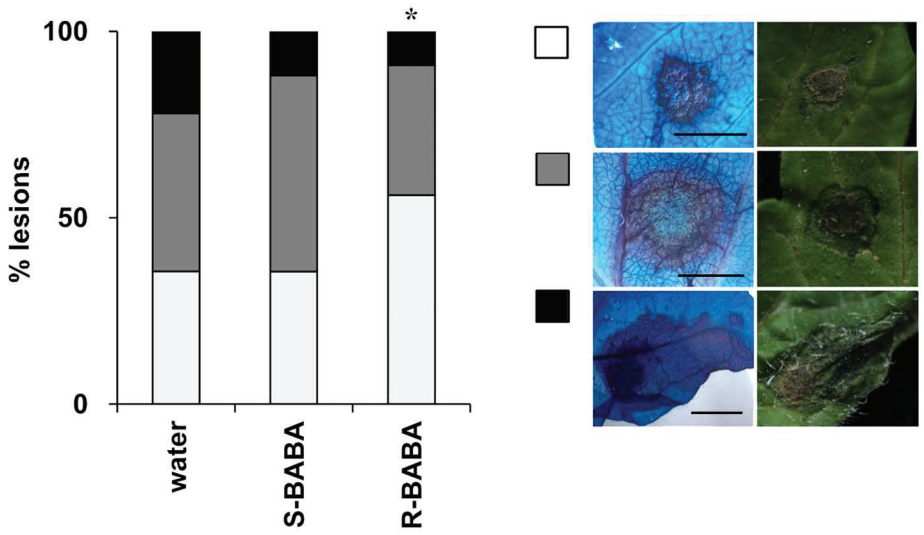

Supplementary Figure 8. Enantiomer-specificity of BABA-induced resistance in tomato against *Botrtis cinerea.* Levels of induced resistance in tomato (cv. Micro-Tom) after root treatment with water, S-BABA (500 µM), or R-BABA (500 µM). Insets show different classes of lesion severity, pathogen colonization and cell death; asterisk indicates a statistically significant difference in class distribution compared to water-treated plants ($\chi 2$ test, $p<0.05$, n=15). Scale bars = 5 mm.

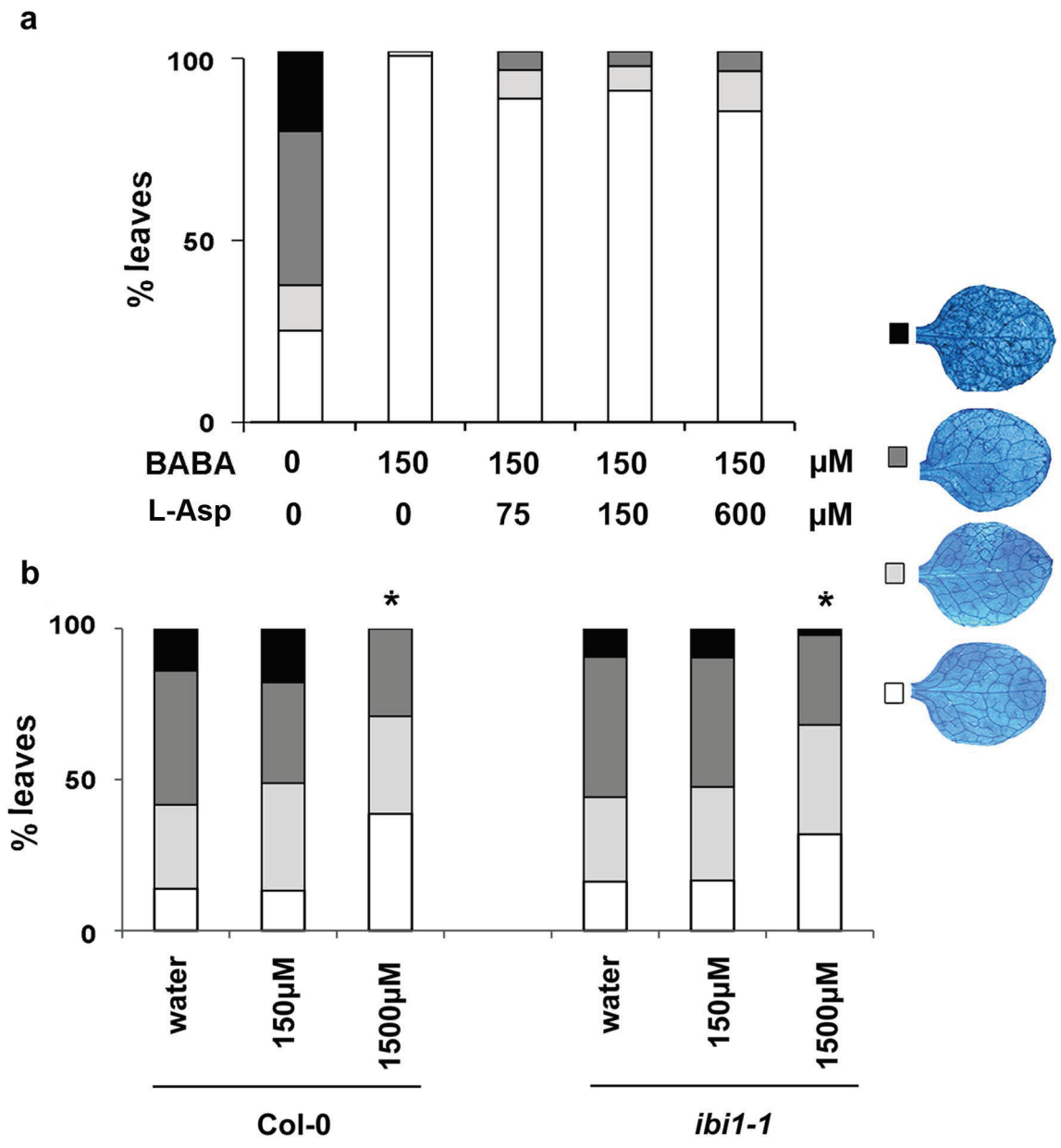

Supplementary Figure 9. (a) Levels of induced resistance against *H. arabidopsidis* WACO9 in Col-0 after co-application of BABA with increasing concentrations of L-Asp to the roots. **(b)** Levels of induced resistance against *H. arabidopsidis* WACO9 (Col-0 and *ibi1-1*) after root treatment with 150 or 1500 µM L-Asp. Insets show different classes of pathogen colonization; asterisks indicate statistically significant differences in class distribution compared to water-treated plants (Fisher's exact test, $p<0.01$, n=50-100).

a

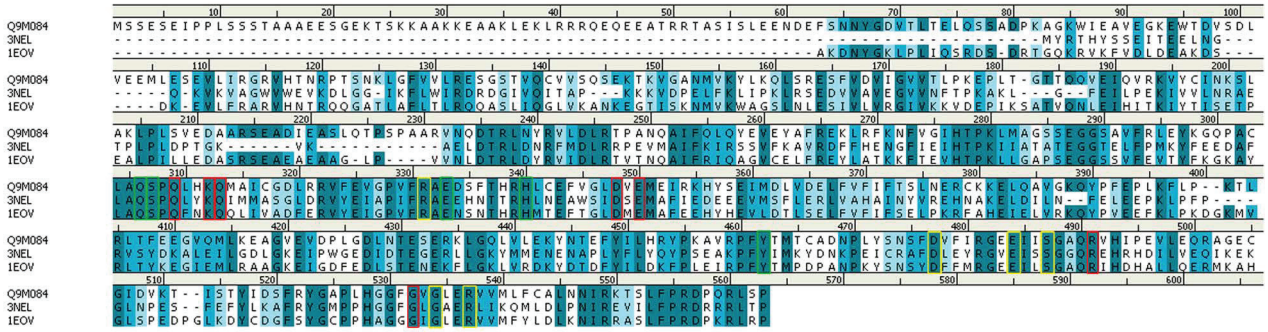

b

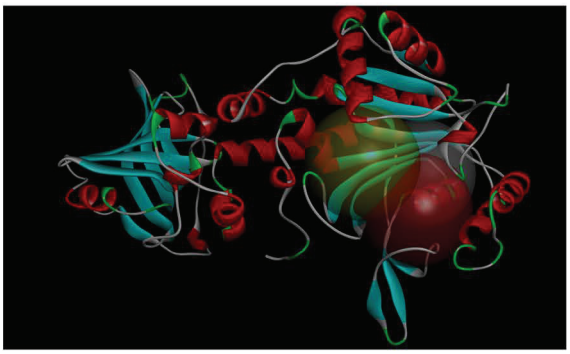

c

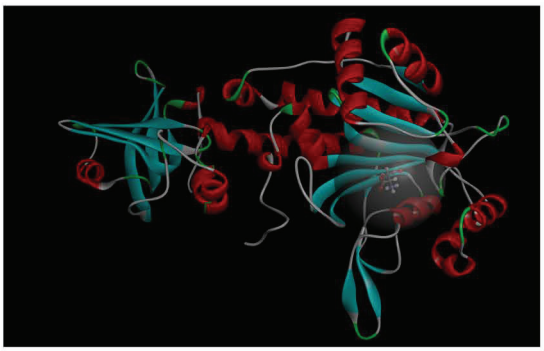

Supplementary Figure 10. Protein models of aspartyl-tRNA synthetase (AspRS) from Arabidopsis, *Pichia pastoris*, and *Pycorcoccus kodakaraensis*. (a) Sequence alignment of Arabidopsis IBI1 (Q9M084; top) with *P. pastoris* AspRS (1EOV; bottom), and *P. kodakaraensis* AspRS (3NEL; middle). Coloured squares highlight conserved residues of binding domains to tRNA (green), ATP (yellow), and L-Asp (red). **(b)** Crystal structure of *P. pastoris* AspRS, highlighting the tRNA-binding site (red sphere), ATP-binding site (yellow sphere) and the L-Asp-binding site (grey sphere). **(c)** Crystal structure of *P. kodakaraensis* AspRS, highlighting the L-Asp binding domain in grey with co-crystallised L-Asp molecule.

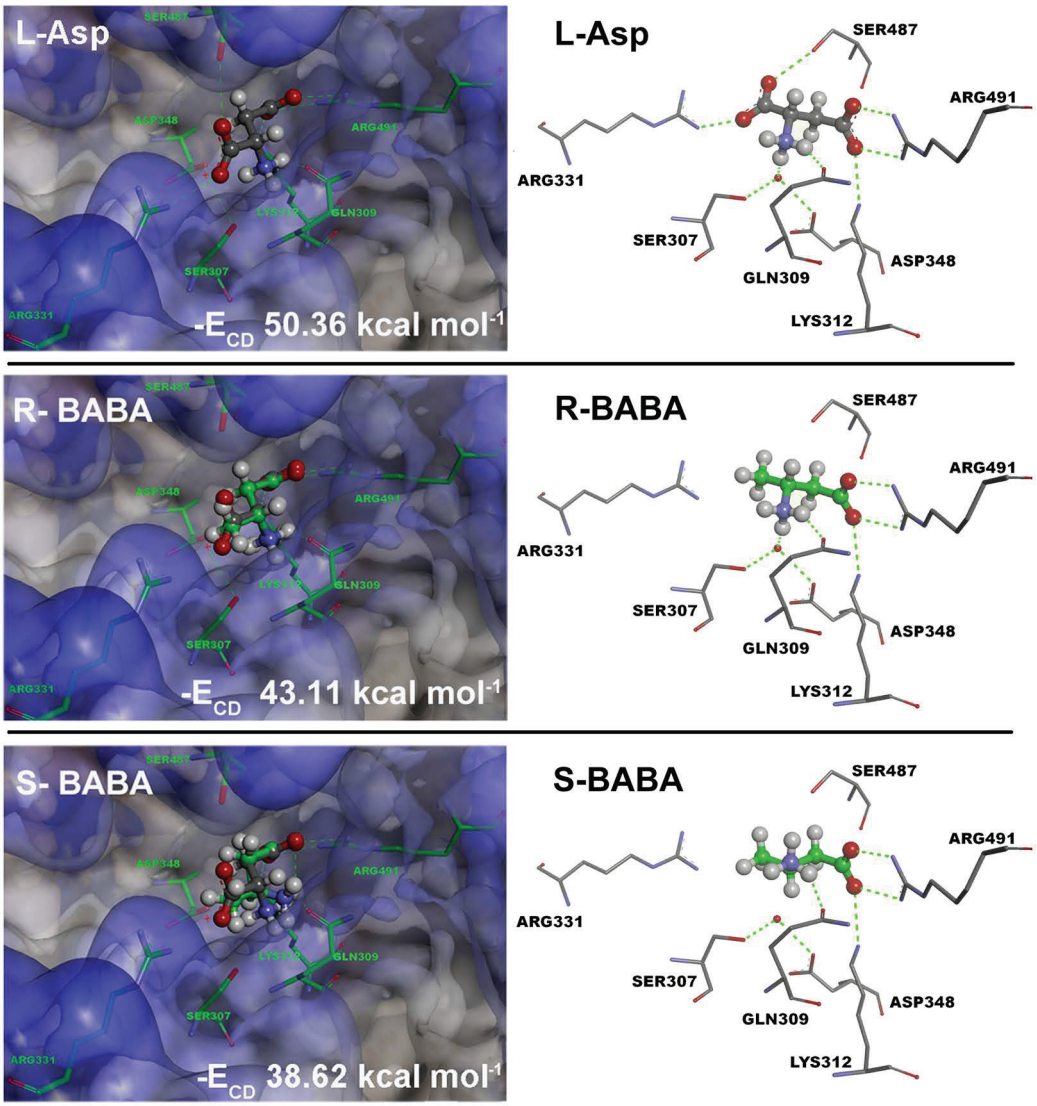

Supplementary Figure 11. Interaction models for binding of L-Asp, R-BABA or S-BABA to the L-Asp binding pocket of *P. kodakaraensis* AspRS. Left panels: 3-D crystal structures of the L-Asp binding pocket of the protein with co-crystallised L-Asp (top; grey), overlaid with a high score docking pose of R-BABA (middle; green) or S-BABA (bottom; green). Numbers indicate CHARMm energy values of the ligand-protein complex. Right panels: 3-D interaction maps showing the key hydrogen bonding interactions between L-Asp (top; grey), R-BABA (middle; green), or S-BABA (bottom; green) with key residues in the binding pocket of AspRS.

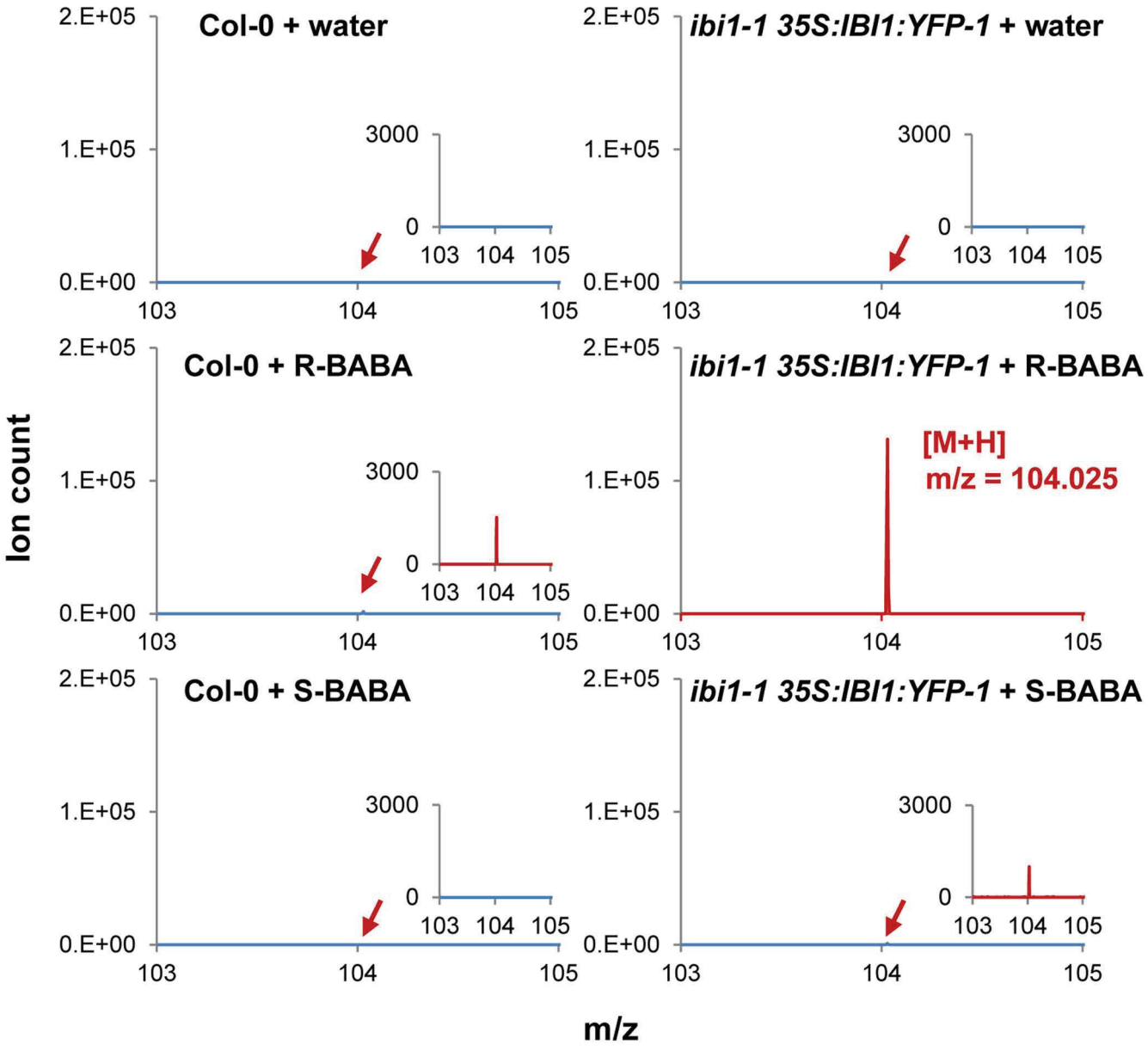

Supplementary Figure 12. Mass spectrometry detection of BABA from immunoprecipitated IBI1:YFP of *ibi1-1 35S:IBI1:YFP-1* or un-transformed Col-0 (negative control), using electrospray ionization coupled to quadrupole-time-of-flight analysis (ESI-qTOF; [M+H]; red arrows indicate intensities at m/z=104,025). Immunoprecipitation (IP) was performed with protein extracts from leaves after two successive root treatments with water (control), R-BABA (1.2 mM), or S-BABA (1.2 mM). ESI-qTOF analysis of IP extracts from *ibi1-1 35S:IBI1:YFP-1* plants after R- or S-BABA applications was repeated twice from material of independent experiments, yielding similar results. Insets show spectra at higher sensitivity.

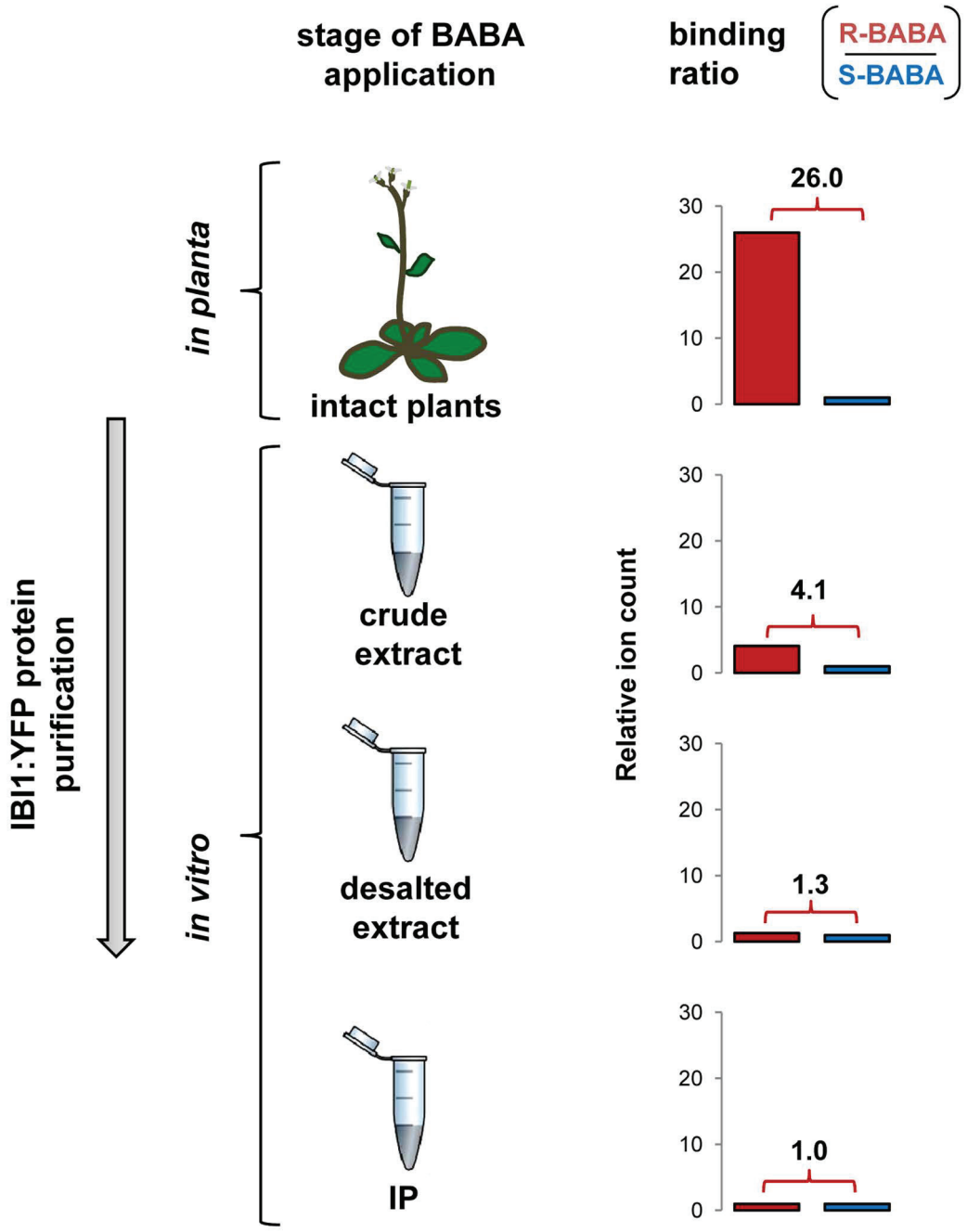

Supplementary Figure 13. Purification of IBI1:YFP from over-expression plants affects enantiomer-specific binding capacity to BABA. When R- and S-BABA are applied to intact *IBI1:YFP-1* plants, the level of BABA retained after immunoprecipitated IBI1:YFP is 26-fold higher from R-BABA-treated plants than from S-BABA-treated plants (see fig. 3b). When the BABA enantiomers are applied to crude protein extract, this binding ratio is reduced to 4.1-fold. When the binding assay is performed with sephadex-purified protein extract and immunoprecipitated IBI1:YFP, the specific binding ratio is reduced further to 1.4 and 1.0, respectively.

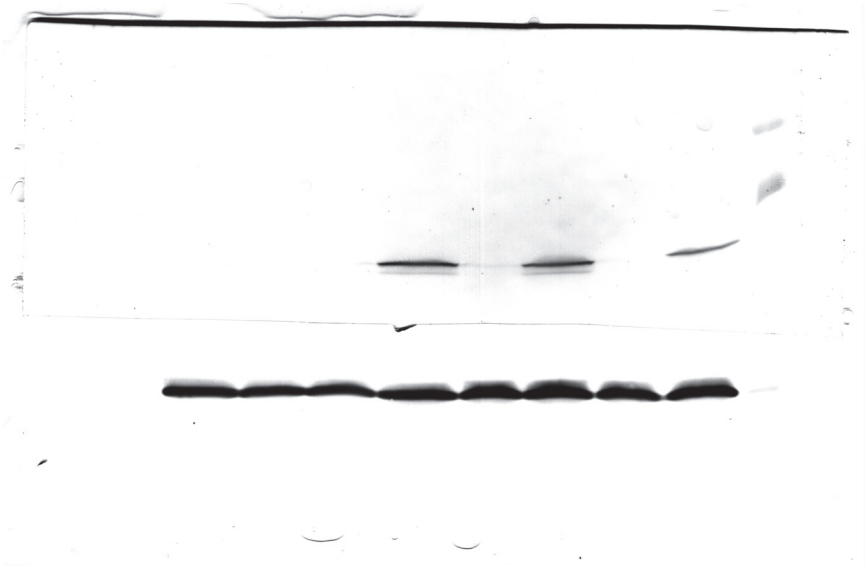

Supplementary Figure 14. Original scans of protein blots of figure 4a.

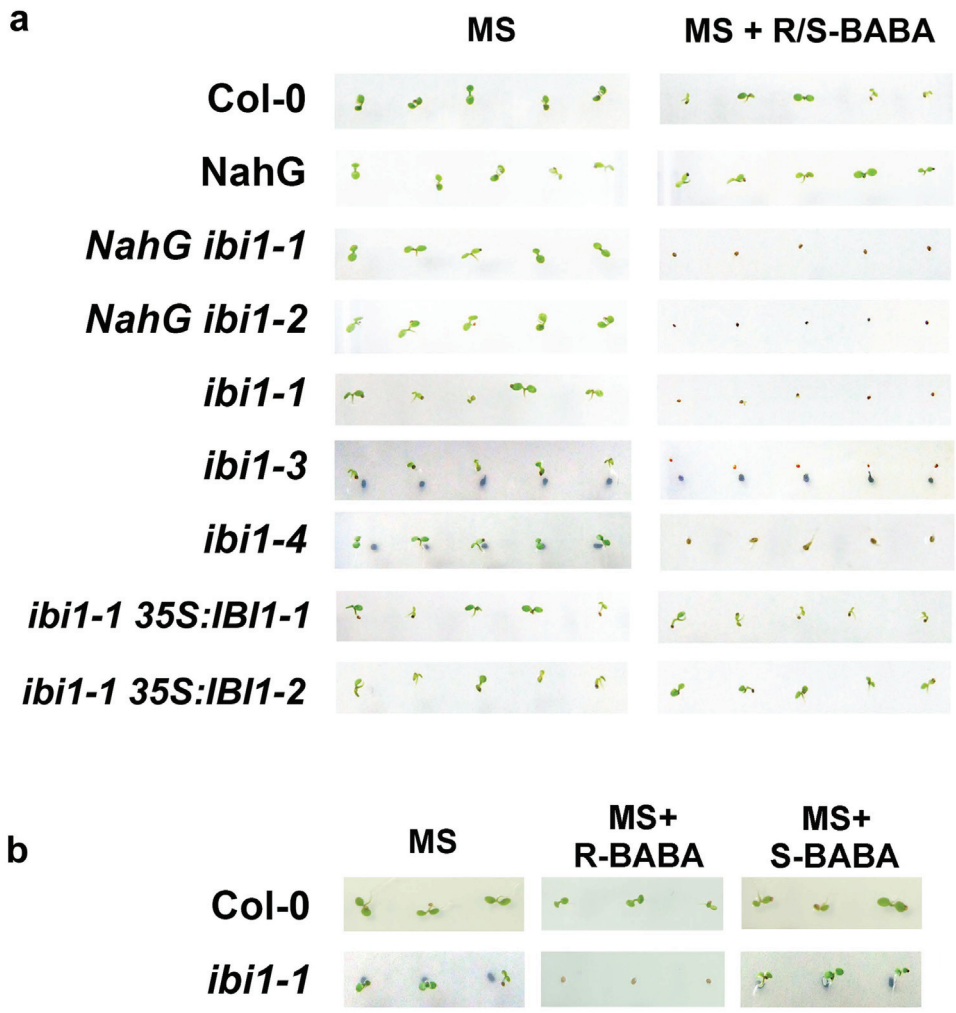

Supplementary Figure 15. Role of IBI1 in BABA-induced stress. (a) Different mutations in *IBI1* block seedling growth on BABA-containing agar (500 µM), which occurs independently from salicylic acid. **(b)** Growth suppression of *ibi1-1* on BABA-containing agar (500 µM) is enantiomer-specific. Photographs show germination rates and seedling growth on ½ strength MS agar medium at 10 days after planting.

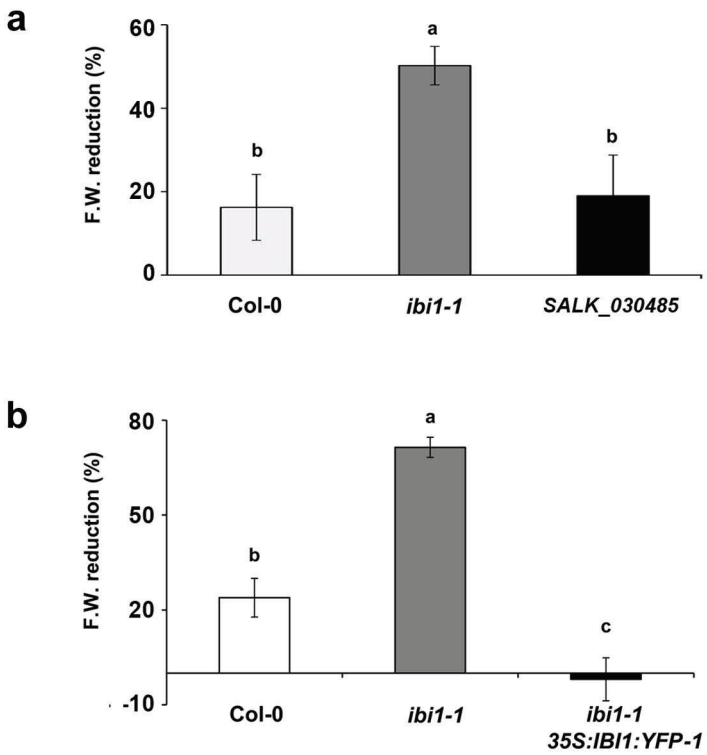

Supplementary Figure 16. Levels of BABA-induced growth suppression at 1 week after root treatment with BABA (400 µM) in **(a)** Col-0, *ibi1-1* and a T-DNA insertion mutant of At4g26870 (*SALK_030485*) and **(b)** Col-0, *ibi1-1* and *ibi1-1 35S:IBI1:YFP-1*. Shown are mean percentages (± SEM, n=15) of fresh weight (F.W.) reduction in BABA-treated plants relative to water-treated plants. Different letters indicate statistically significant differences between genotypes (Fisher's least significant differences test; $p<0.05$).

Supplementary Table 1: Experimental details of i*n vitro* AspRS activity assays.

Substrate				Reaction buffer								Conditions		Reference
L-asp (mM)	ATP (mM)	$tRNA^{Asp}$ (ng/µl)	Crude tRNA wheat germ (µg/ml)	HEPES (mM)	Tris-HCl pH 7.8 (mM)	BSA (%)	Spermine (mM)	MgCl2 (mM)	NaCl (mM)	KCl (mM)	DTT (mM)	T (°C)	Lenght (mins.)	
2	2	_	_	_	100	0.05	_	10	_	_	_	37	30	[36]
2	1	100	_	_	25	0.05	1	0.2	_	_	0.1	37	30	[37]
2	0.2	80	_	30	_	_	_	10	140	30	5	23	60	[38]
2	0.2	80	_	30	_	_	_	10	140	30	1	23	15	
2	0.2	80	_	30	_	_	_	10	140	30	1	37	15	
2	0.2	_	0	30	_	_	_	10	140	30	1	37	15	
2	0.2	_	8	30	_	_	_	10	140	30	1	37	15	
2	0.2	_	80	30	_	_	_	10	140	30	1	37	15	
2	0.2	_	800	30	_	_	_	10	140	30	1	37	15	
2	0.2	_	0	30	_	_	_	10	140	30	1	23	60	
2	0.2	_	8	30	_	_	_	10	140	30	1	23	60	
2	0.2	_	80	30	_	_	_	10	140	30	1	23	60	
2	0.2	_	800	30	_	_	_	10	140	30	1	23	60	
2	0.2	80	_	30	_	_	_	10	140	30	1	37	30	[39]

Supplementary Table 2. Arabidopsis genotypes, backgrounds, origins, and/or PCR primers used for selection.

Genotype	Background	Origin	PCR primers
NahG B15	Col-0	34	Fw: ACTCTGCCGCTACTCCCATA Rv: CGAGCCCTAGGTACATCTGC
NahG *ibi1-1*	NahG B15	Mutant Screen	
NahG *ibi1-2*	NahG B15	Mutant Screen	
ibi1-1	Col-0	Mutant screen	*IBI1* FW:GGATCCGAAAGCCGGGAAGTTG *ibi1-1* FW: GGATCCGAAAGCCGGGAAGTTA Rv : AAACCTGCTGCGTAGTTCCCGTCAG
ibi1-3	Col-0	SALK-103893	LP: TTGGATTCTGATAATCGGCAC RP: TGATCAGTGATCACAGCAACC
ibi1-4	Col-0	SAIL-228-H03	LP TGACTTGTGCCGATAATCCTC RP TTAACGCTTCTGTTCCACCAC
ibi1-hm	Col-0	SALK_030485	NASC ID: N656329
gcn2	L*er*	43	NASC ID: N656329